Supplementary material for "Inference of intensity based models for load-sharing systems with damage accumulation"

Christine H. Müller* and Renate Meyer†

November 26, 2020

Further results concerning the Bayesian analysis are presented in Section 1. Further frequentist confidence sets and Bayesian credible sets and details of their calculation are given in Section 2, and details concerning the calculation of the prediction intervals are given in Section 3. In Section 3 also the difference between prediction intervals based on credible sets and the classical Bayesian prediction intervals is outlined and it is explained why the classical Bayesian prediction intervals cannot be used easily in the models with damage accumulation. Sections 4 and 5 provide further results of the simulation study. Since the estimates differs if they were calculated in the scale invariant or the scale dependent version, Section 6 explains how one version can be transformed into the other version. More details of the proofs are given in Section 7.

1 Further results of the Bayesian analysis

Traceplots and kernel density estimates of the marginal posterior distributions of each parameter for each of the three models are given in Figures 1, 2, 3 and 4. Figure 3 illustrates the problem of sampling the posterior distribution in the model with additive damage accumulation. Here the two MCMC chains with different initial values get stuck in one of two local maxima.

*Department of Statistics, TU Dortmund University, D-44227 Dortmund, Germany, cmueller@statistik.tu-dortmund.de

†Department of Statistics, University of Auckland, New Zealand

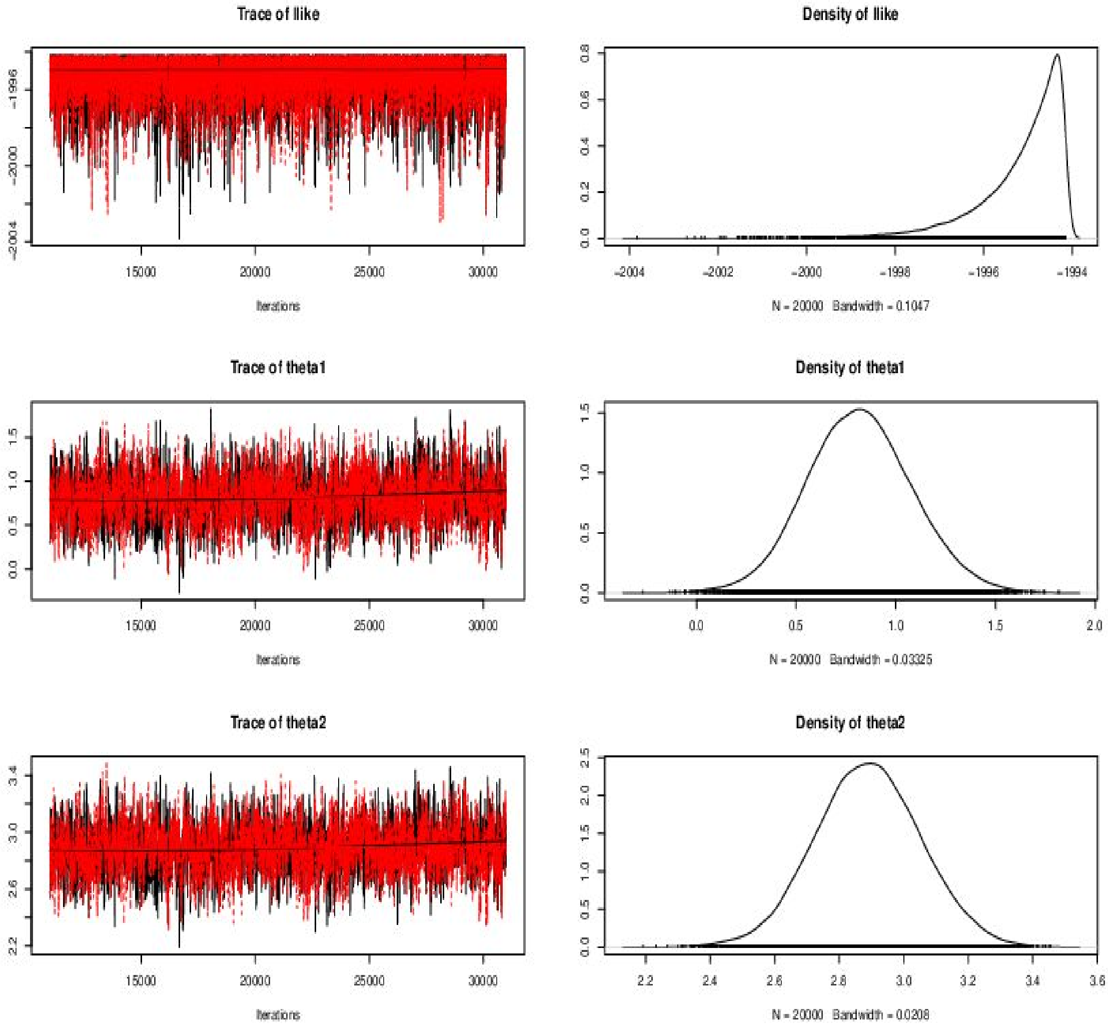

Figure 1: Traceplots and kernel density estimates for the parameters of the load sharing model without damage accumulation.

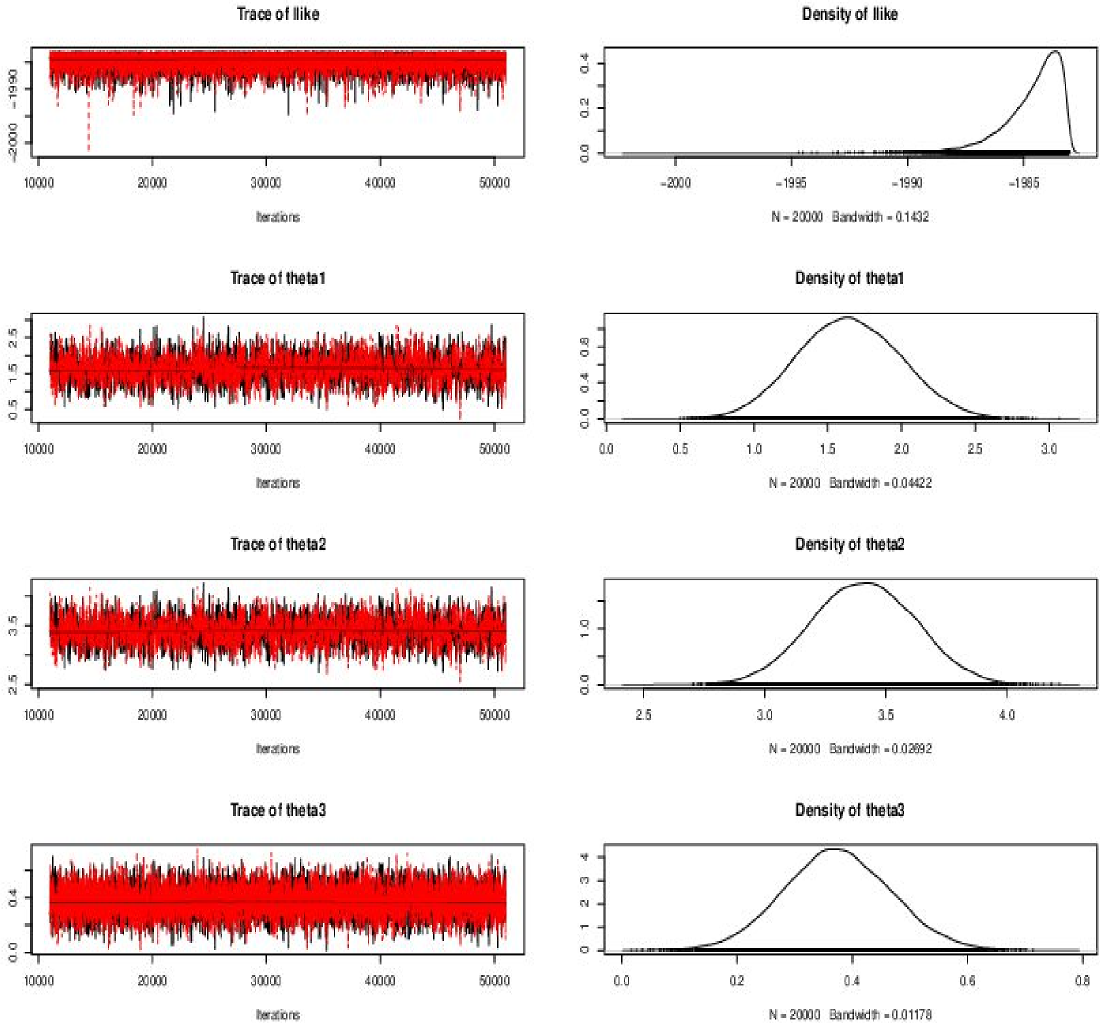

Figure 2: Traceplots and kernel density estimates for the parameters of the load sharing model with multiplicative damage accumulation.

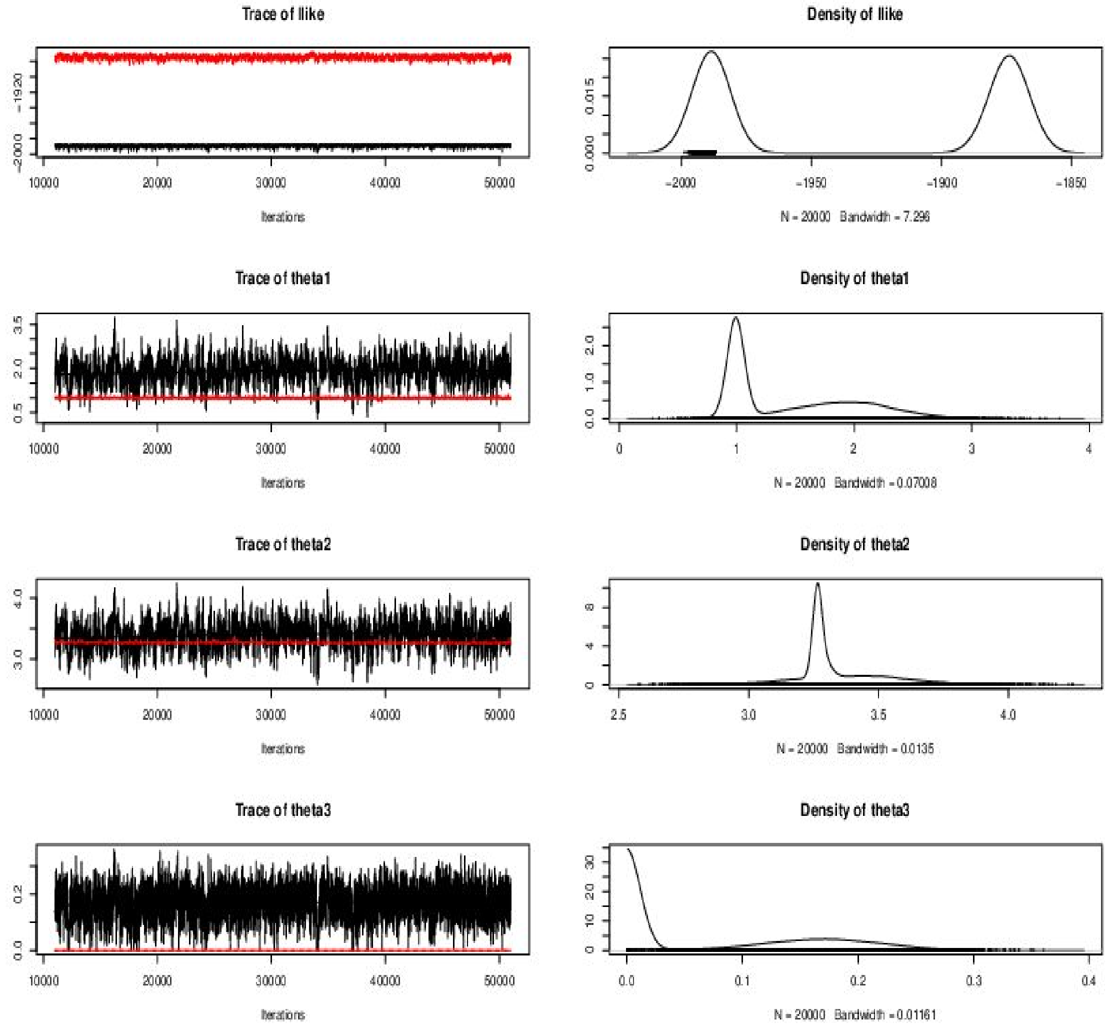

Figure 3: Traceplots and kernel density estimates for the parameters of the load sharing model with additive damage accumulation from two chains with different starting values.

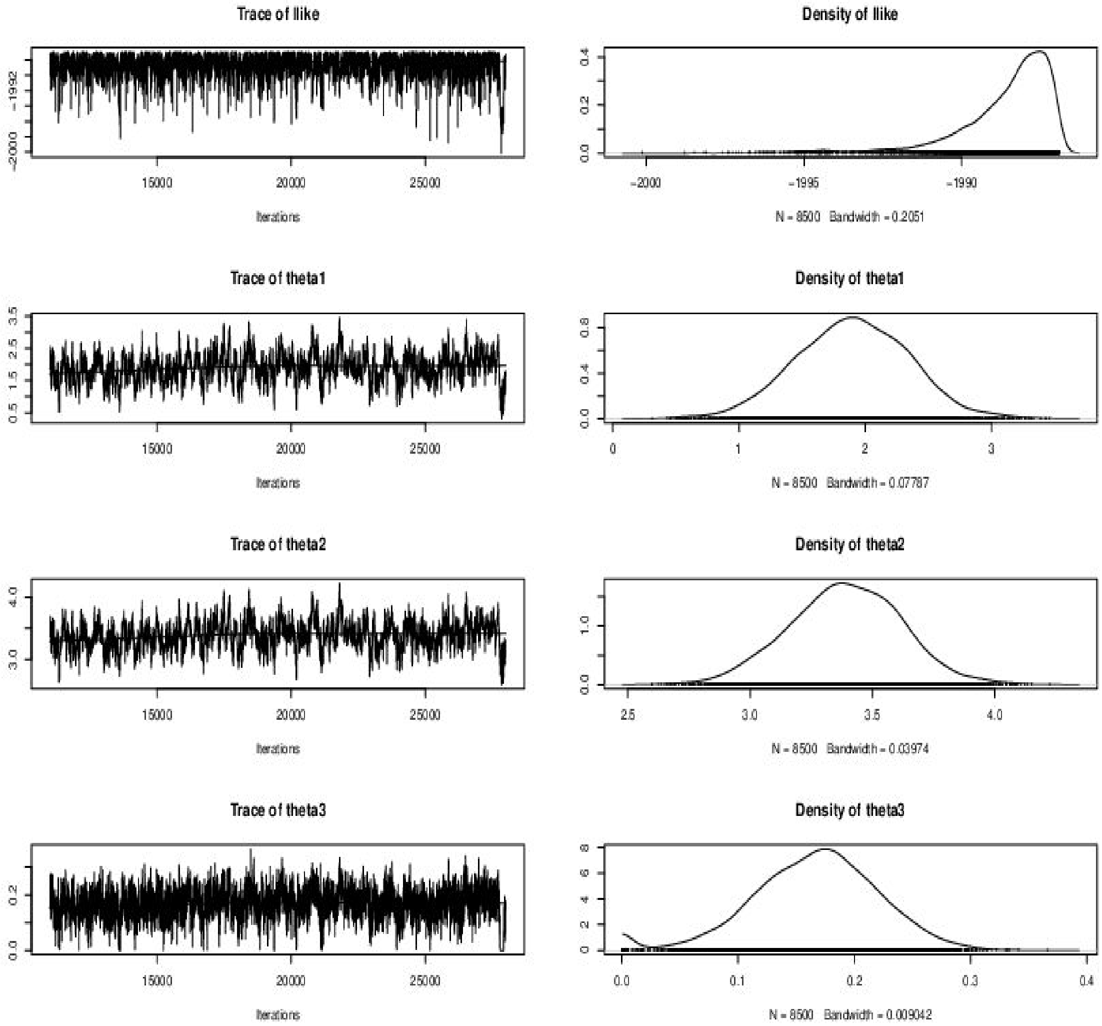

Figure 4: Traceplots and kernel density estimates for the parameters of the load sharing model with additive damage accumulation.

2 Further frequentist confidence sets and Bayesian credible sets and details of their calculation

To calculate the 90%-prediction intervals in the case of the models with multiplicative and additive damage accumulation, 95%-confidence sets were calculated via grids with 101^3 points. The 101^3 grid points were distributed with equidistant steps in $[3.8, 8.2] \times [2.4, 4.3] \times [0, 0.8]$ for the model with multiplicative damage accumulation and in $[3.4, 6.6] \times [2.5, 4.3] \times [0.0001, 0.016]$ for the model with additive damage accumulation. To make a fair comparison, the confidence set for the model without damage accumulation were determined by a grid with 101^2 points lying in $[2.8, 5.0] \times [2.1, 3.5]$. All these grids contain at the border points which are not included in the confidence sets so that the grids were large enough. Moreover, the grids were also not too large since the obtained confidence set for multiplicative damage accumulation contains 18 062 points, the one for additive damage accumulation 34 384 points, and the one for the model without damage accumulation 21 300 points. The 95%-credible sets for Bayesian analysis were obtained by using the 40 000 simulated parameters of the posterior distribution for the model without and with multiplicative damage accumulation and the 8 500 simulated parameters of the model with additive damage accumulation. Using Tukey's half space depth led in all three models to the smallest sets with at least 95% of the simulated parameters of the posterior distribution. This resulted in a set of 38 007 parameters with a half space depth greater than 0.002974987 for the model with multiplicative damage accumulation, in a set of 8 079 parameters with a half space depth greater than 0.00635294 for the model with additive damage accumulation, and in a set of 38 009 parameters with a half space depth greater than 0.007124996 for the model without damage accumulation.

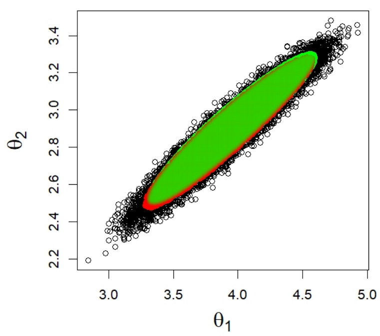

Figure 5: The whole set of simulated parameters of the posterior distribution (black), the frequentist 95%-confidence sets (green) and the Bayesian 95%-credible sets (red) for the model without damage accumulation in the scale dependent version with $\tau_\star = 10^6$.

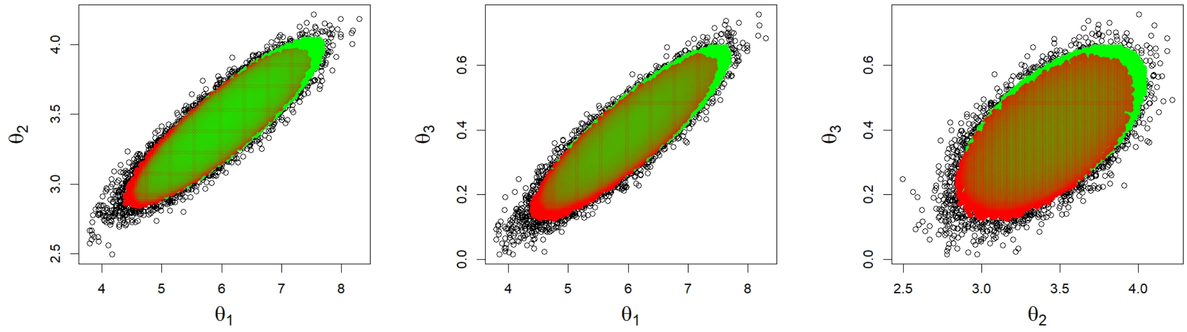

Figure 6: Two-dimensional projections of the whole set of simulated parameters of the posterior distribution (black), the frequentist 95%-confidence sets (green) and the Bayesian 95%-credible sets (red) for the model with multiplicative damage accumulation in the scale dependent version with $\tau_\star = 10^6$.

3 Details of the calculation of the prediction intervals

Hereinafter, $D = M, A, W$ denotes the model with multiplicative, additive and without damage accumulation, respectively. Recall that the frequentist asymptotic $(1-\alpha)$-prediction interval $\mathbb{P}^F_{D,1-\alpha}$ for the future failure time $T^D_{I_c,0}$ is given by

$$\mathbb{P}^F_{D,1-\alpha} := \bigcup_{\theta \in \mathbb{C}^F_{D,1-\alpha/2}} \left[q^D_{\alpha/4}(\theta), q^D_{1-\alpha/4}(\theta)\right], \tag{1}$$

where $\mathbb{C}^F_{D,1-\alpha/2}$ is a $(1-\alpha/2)$-confidence set of θ while the Bayesian $(1-\alpha)$-prediction interval $\mathbb{P}^B_{D,1-\alpha}$ for $T^D_{I_c,0}$ is given by

$$\mathbb{P}^B_{D,1-\alpha} := \bigcup_{\theta \in \mathbb{C}^B_{D,1-\alpha/2}} \left[q^D_{\alpha/4}(\theta), q^D_{1-\alpha/4}(\theta)\right], \tag{2}$$

where $\mathbb{C}^B_{D,1-\alpha/2}$ is the credible set. Both prediction intervals are based on the quantiles $q^D_{\alpha/4}(\theta)$ and $q^D_{1-\alpha/4}(\theta)$ of the distribution of the future failure time $T^D_{I_c,0}$.

For calculating the 90%-prediction intervals, each of the calculated 95%-confidence sets and 95%-credible sets were thinned to approximately 2 000 parameters. Then, the thinned confidence set for the model with multiplicative damage accumulation includes 10% of the original 18 062 parameters, the thinned confidence set for the model with additive damage accumulation includes 5% of the 34 384 parameters, and the thinned confidence set for the model without damage accumulation includes 10% of the original 21 300 parameters. Similarly, the thinned credible set for the model with multiplicative damage accumulation includes 5% of the original 38 007 parameters, the thinned credible set for the model with additive damage accumulation includes 20% of the 38 079 parameters, and the thinned credible set for the model without damage accumulation includes 5% of the original 38 009 parameters. Then 10 000 point processes were simulated for each parameter of the thinned versions of the confidence sets and credible sets. The predictive distribution of the time of the I_cth break is approximated by the 10 000 time points of the I_cth event in these 10 000 point processes. Using the 0.025-quantile and the 0.975-quantile of the 10 000 time points of the I_cth event provides then the intervals $\left[q^D_{\alpha/4}(\theta), q^D_{1-\alpha/4}(\theta)\right]$ in (1) and (2) for $\alpha = 0.1$.

Because of the thinning, the prediction intervals are slightly too short. On the other hand, the prediction intervals are slightly too large. Namely, for simplicity and to use them for Experiment SB06 as well as for Experiment SB06a, the 95%-confidence sets and 95%-credible sets were based only on $\mathbf{N} = \{N_j(t)_{t\le\tau_j};\ j = 1, \dots, J\}$ and not on $\mathbf{N}_0 = \{N_j(t)_{t\le\tau_j};\ j = 0, 1, \dots, J\}$. To include the general case in the proof of Lemma III.1 and Lemma III.2, it was assumed that the confidence sets and credible sets are of form $\mathbb{C}(\boldsymbol{\mathcal{N}}_0)$, but the proof holds also for $\mathbb{C}(\boldsymbol{\mathcal{N}})$. Since $\mathbb{C}(\boldsymbol{\mathcal{N}})$ is larger than $\mathbb{C}(\boldsymbol{\mathcal{N}}_0)$, the prediction intervals becomes only larger. However, we have then independence of $\{T \in \mathbb{P}(\theta, \boldsymbol{\mathcal{N}}_0)\}$ and $\mathbb{C}(\boldsymbol{\mathcal{N}})$ since the predictive interval $\mathbb{P}(\theta, \boldsymbol{\mathcal{N}}_0) = \left[q^D_{\alpha/4}(\theta), q^D_{1-\alpha/4}(\theta)\right]$ depends only on $\mathcal{N}_0(t)_{t\le\tau_0}$. This means that the level of the prediction interval can be determined as in Leckey et al. (2020) and is $(1 - \frac{\alpha}{2})^2$ instead of $(1 - \alpha)$ with $\alpha = 0.1$. Nevertheless, the results for the model without damage accumulation are very similar to those of Leckey et al. (2020).

It should also be noted here that usually the posterior predictive distribution of $T := T_{I_c,0}$ given $\boldsymbol{\mathcal{N}}_0 = \mathbf{N}_0$ is obtained by

$$\begin{aligned} p_{T|\boldsymbol{\mathcal{N}}_0=\mathbf{N}_0}(t) =: p(t|\mathbf{N}_0) &= \frac{p(t, \mathbf{N}_0)}{p(\mathbf{N}_0)} = \frac{1}{p(\mathbf{N}_0)} \int p(t, \mathbf{N}_0, \theta)\, d\theta \\ = \ \frac{1}{p(\mathbf{N}_0)} \int p(t|\mathbf{N}_0, \theta)\, p(\mathbf{N}_0, \theta)\, d\theta &= \int p(t|\mathbf{N}_0, \theta)\, p(\theta|\mathbf{N}_0)\, d\theta. \end{aligned}$$

A sample from this posterior predictive distribution can be obtained by sampling a t_k from the likelihood $p(t|\mathbf{N}_0, \theta^{(k)})$ for each sample $\theta^{(k)}$ from the posterior distribution. The problem is that the distribution of T given $(\boldsymbol{\mathcal{N}}_0, \Theta) = (\mathbf{N}_0, \theta)$, which has the density $p(t|\mathbf{N}_0, \theta)$, has no simple form. Only for the model without damage accumulation, it has a simple form since it is the hypoexponential distribution so that it can be easily sampled. Therefore, we decided to obtain an approximate posterior prediction interval by an analogous procedure to the frequentist prediction interval consistently for the models with and without damage accumulation.

4 Further results of the simulation study for the estimators

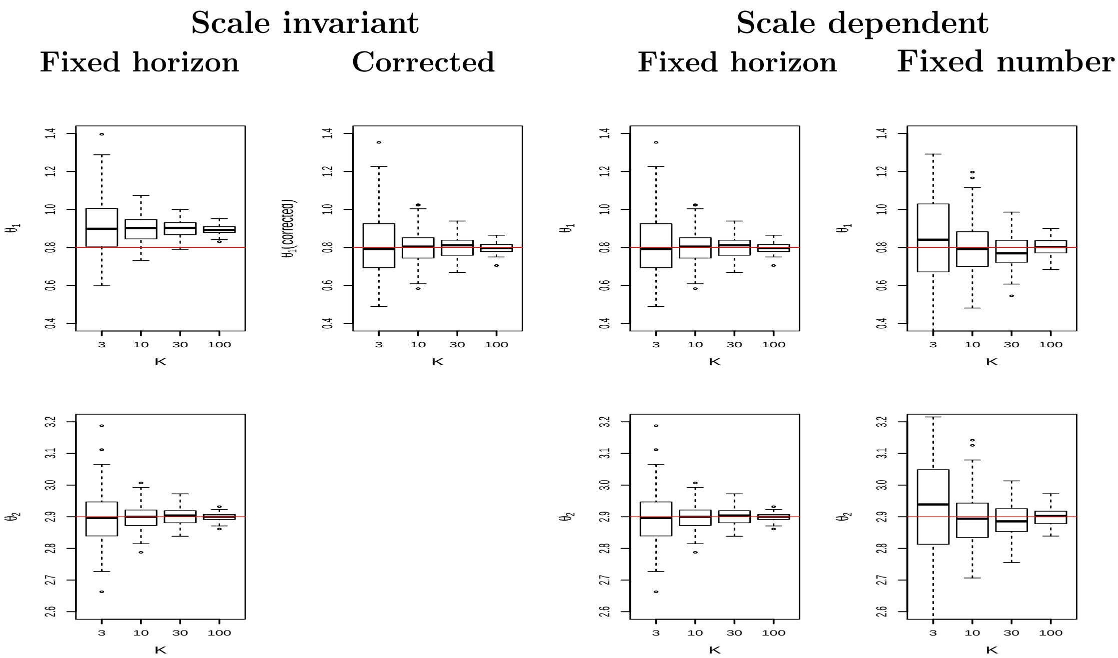

Figure 7: Boxplots of the estimates for $\theta = (\theta_1, \theta_2)^\top$ for the simulated load sharing model without damage accumulation. First column: scale invariant estimator in the scenario of fixed horizon. Second column: correction of the scale invariant estimator. Third column: scale dependent estimator in the scenario of fixed horizon. Fourth column: scale dependent estimator in the scenario of fixed number of failures. The red line marks the true parameter. The number of repetitions was 100.

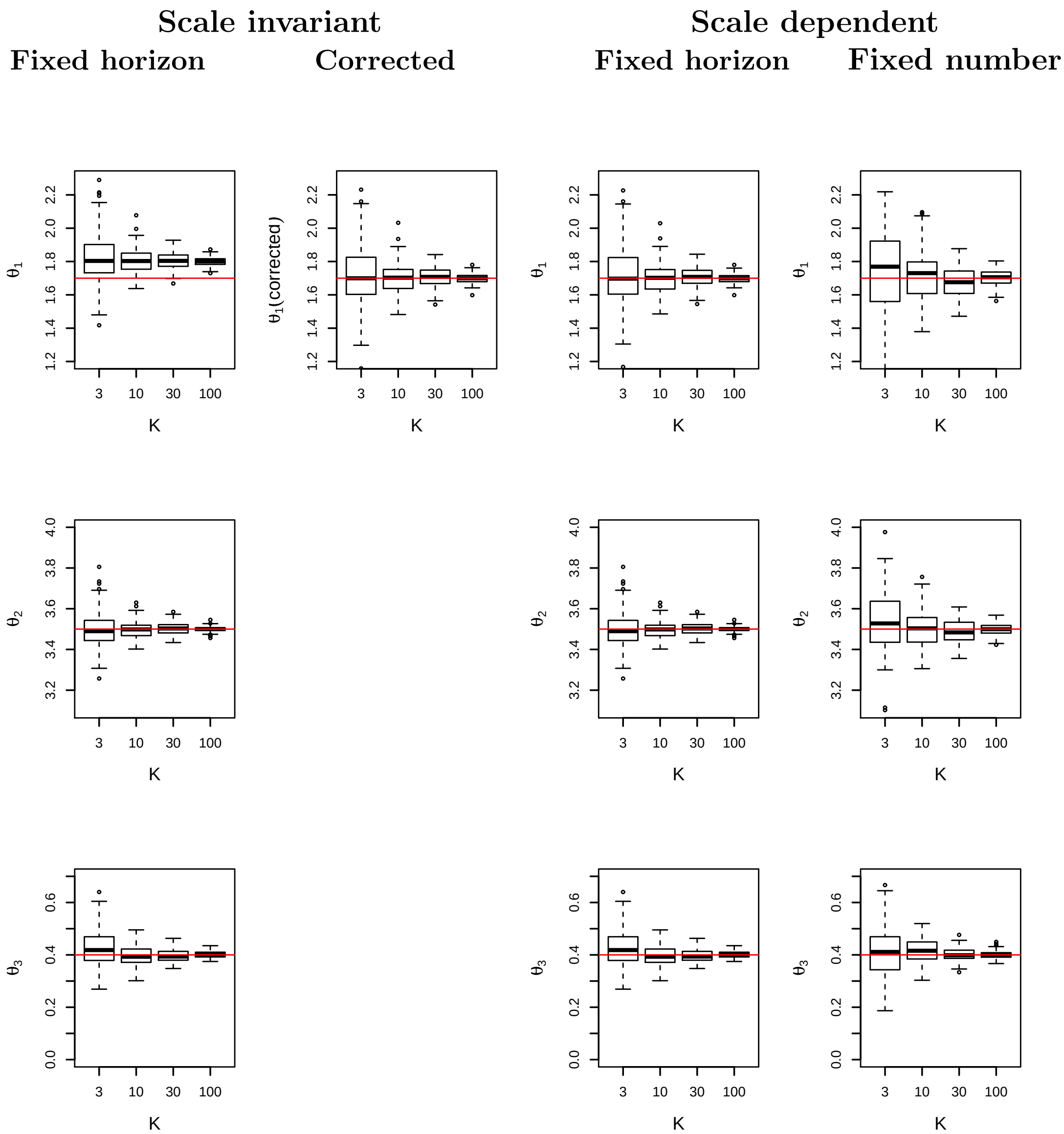

Figure 8: Boxplots of the estimates for $\theta = (\theta_1, \theta_2, \theta_3)^\top$ for the simulated load sharing model with multiplicative damage accumulation. First column: scale invariant estimator in the scenario of fixed horizon. Second column: correction of the scale invariant estimator. Third column: scale dependent estimator in the scenario of fixed horizon. Fourth column: scale dependent estimator in the scenario of fixed number of failures. The red line marks the true parameter. The number of repetitions was 100.

5 Further results of the simulation study for the tests

Figure 9 and Figure 10 provide further simulation results concerning the rejection rates under the null hypothesis of the likelihood ratio test for $H_0 : \theta = \theta_*$ and the likelihood ratio test for testing the null hypothesis of no multiplicative damage accumulation and no additive damage accumulation, respectively, for growing sample size for the scenarios with fixed time horizon (left column) and fixed number of failures (right column). With 1 000 simulations, the variability of the rejection rates are still high, which can be seen also by the repetition of the simulation study with different random numbers in the second row. In particular, Figure 10 demonstrates that the tests for no damage accumulation are too conservative.

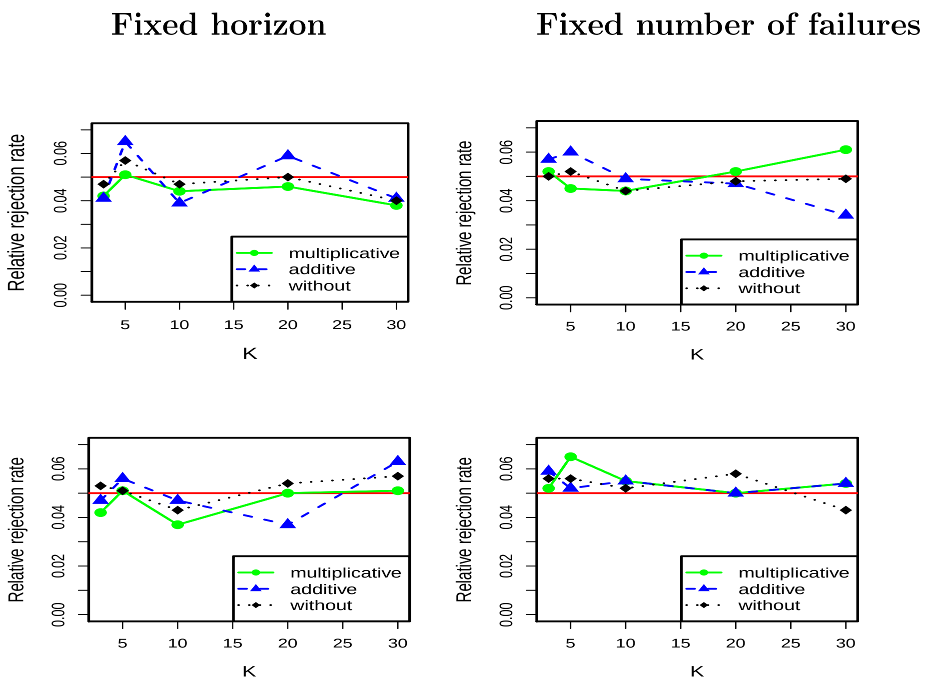

Figure 9: Rejection rates of the likelihood ratio test for testing the null hypothesis $H_0 : \theta = \theta_*$ in the models with multiplicative damage accumulation, additive damage accumulation, and without damage accumulation. First column: scenario with fixed horizon. Second column: scenario with fixed number of failures. Second row: results with different random numbers. The red line marks the test level of 0.05. The number of repetitions was 1 000.

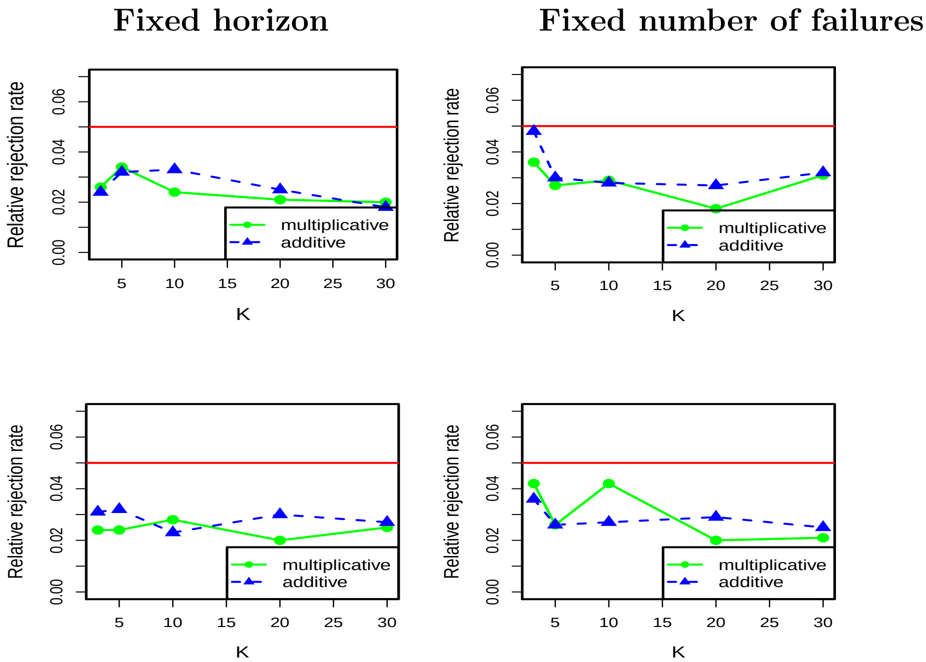

Figure 10: Rejection rates of the likelihood ratio test for testing the null hypothesis $H_0 : \theta_3 = 0$ in the models with multiplicative damage accumulation and additive damage accumulation for different values of K. First column: scenario with fixed horizon. Second column: scenario with fixed number of failures. Second row: results with different random numbers. The red line marks the test level of 0.05. The number of repetitions was 1 000.

6 Transformation of parameters

The likelihood functions are dependent of the parameter τ for adjusting for different time scales. The likelihood functions are given in a form that is numerical stable. However, if different values for τ are used than the following representations are useful:

For the multiplicative model, we have

$$
\begin{aligned}
&\ln(L_M((\theta_1(\tau), \theta_2(\tau), \theta_3(\tau))^\top)) \\
= \;& \sum_{j=1}^{J} \left\{ \sum_{i=1}^{I^j} \left[-\theta_1(\tau) + \theta_2(\tau)\ln(a_{ij}) + \theta_3(\tau)\ln\left(\frac{1}{\tau}C_j(i)\right) - \ln(\tau) \right] \right. \\
& \left. - \frac{\exp(-\theta_1(\tau))}{\theta_3(\tau)+1} \left[\sum_{i=1}^{I^j+1} a_{ij}^{\theta_2(\tau)-1} \left(\left(\frac{1}{\tau}C_j(i)\right)^{\theta_3(\tau)+1} - \left(\frac{1}{\tau}C_j(i-1)\right)^{\theta_3(\tau)+1} \right) \right] \right\} \\
= \;& \sum_{j=1}^{J} \left\{ \sum_{i=1}^{I^j} \left[-\theta_1(\tau) + \theta_2(\tau)\ln(a_{ij}) + \theta_3(\tau)\ln(C_j(i)) - \theta_3(\tau)\ln(\tau) - \ln(\tau) \right] \right. \\
& \left. - \frac{\exp(-\theta_1(\tau))}{\theta_3(\tau)+1} \left[\sum_{i=1}^{I^j+1} a_{ij}^{\theta_2(\tau)-1} \left(\frac{1}{\tau}\right)^{\theta_3(\tau)+1} \left(C_j(i)^{\theta_3(\tau)+1} - C_j(i-1)^{\theta_3(\tau)+1} \right) \right] \right\} \\
= \;& \sum_{j=1}^{J} \left\{ \sum_{i=1}^{I^j} \left[-\left\{\theta_1(\tau) + (\theta_3(\tau)+1)\ln(\tau)\right\} + \theta_2(\tau)\ln(a_{ij}) + \theta_3(\tau)\ln(C_j(i)) \right] \right. \\
& \left. - \frac{\exp(-\left\{\theta_1(\tau) + (\theta_3(\tau)+1)\ln(\tau)\right\})}{\theta_3(\tau)+1} \left[\sum_{i=1}^{I^j+1} a_{ij}^{\theta_2(\tau)-1} \left(C_j(i)^{\theta_3(\tau)+1} - C_j(i-1)^{\theta_3(\tau)+1} \right) \right] \right\} \\
= \;& \sum_{j=1}^{J} \left\{ \sum_{i=1}^{I^j} \left[-\theta_1 + \theta_2\ln(a_{ij}) + \theta_3\ln(C_j(i)) \right] \right. \\
& \left. - \frac{\exp(-\theta_1)}{\theta_3+1} \left[\sum_{i=1}^{I^j+1} a_{ij}^{\theta_2-1} \left(C_j(i)^{\theta_3+1} - C_j(i-1)^{\theta_3+1} \right) \right] \right\}
\end{aligned}
$$

with $\theta_1 := \theta_1(\tau) + (\theta_3(\tau)+1)\ln(\tau)$, $\theta_2 := \theta_2(\tau)$, and $\theta_3 := \theta_3(\tau)$. The last representation is a version not depending on τ. However, it can be numerically instable because of large values of C_j. Hence for different τ_0 and τ_* we get

$$
\begin{aligned}
&\theta_2(\tau_0) = \theta_2 = \theta_2(\tau_*),\; \theta_3(\tau_0) = \theta_3 = \theta_3(\tau_*), \\
&\theta_1(\tau_0) + (\theta_3+1)\ln(\tau_0) = \theta_1 = \theta_1(\tau_*) + (\theta_3+1)\ln(\tau_*) \\
&\Leftrightarrow \theta_1(\tau_0) = \theta_1(\tau_*) + (\theta_3+1)[\ln(\tau_*) - \ln(\tau_0)].
\end{aligned}
$$

For the additive model, we get

$$\ln(L_A((\theta_1(\tau), \theta_2(\tau), \theta_3(\tau))^\top))$$

$$
\begin{aligned}
= \; & \sum_{j=1}^{J}\left\{\sum_{i=1}^{I^j}\left[-\theta_1(\tau)+\theta_2(\tau)\ln\left(a_{ij}+\frac{\theta_3(\tau)}{\tau}C_j(i)\right)-\ln(\tau)\right]\right. \\
- \; & \frac{\exp(-\theta_1(\tau))}{\theta_3(\tau)(\theta_2(\tau)+1)}\left[\sum_{i=1}^{I^j+1}\frac{1}{a_{ij}}\left(\left(a_{ij}+\frac{\theta_3(\tau)}{\tau}C_j(i)\right)^{\theta_2(\tau)+1}\right.\right. \\
& \qquad\qquad \left.\left.\left.-\left(a_{ij}+\frac{\theta_3(\tau)}{\tau}C_j(i-1)\right)^{\theta_2(\tau)+1}\right)\right]\right\} \\
= \; & \sum_{j=1}^{J}\left\{\sum_{i=1}^{I^j}\left[-\theta_1(\tau)+\theta_2(\tau)\ln\left(a_{ij}+\frac{\theta_3(\tau)}{\tau}C_j(i)\right)-\ln(\tau)\right]\right. \\
- \; & \frac{\exp(-\theta_1(\tau))\frac{1}{\tau}}{\frac{\theta_3(\tau)}{\tau}(\theta_2(\tau)+1)}\left[\sum_{i=1}^{I^j+1}\frac{1}{a_{ij}}\left(\left(a_{ij}+\frac{\theta_3(\tau)}{\tau}C_j(i)\right)^{\theta_2(\tau)+1}\right.\right. \\
& \qquad\qquad \left.\left.\left.-\left(a_{ij}+\frac{\theta_3(\tau)}{\tau}C_j(i-1)\right)^{\theta_2(\tau)+1}\right)\right]\right\} \\
= \; & \sum_{j=1}^{J}\left\{\sum_{i=1}^{I^j}\left[-\{\theta_1(\tau)+\ln(\tau)\}+\theta_2(\tau)\ln\left(a_{ij}+\frac{\theta_3(\tau)}{\tau}C_j(i)\right)\right]\right. \\
- \; & \frac{\exp(-\{\theta_1(\tau)+\ln(\tau)\})}{\frac{\theta_3(\tau)}{\tau}(\theta_2(\tau)+1)}\left[\sum_{i=1}^{I^j+1}\frac{1}{a_{ij}}\left(\left(a_{ij}+\frac{\theta_3(\tau)}{\tau}C_j(i)\right)^{\theta_2(\tau)+1}\right.\right. \\
& \qquad\qquad \left.\left.\left.-\left(a_{ij}+\frac{\theta_3(\tau)}{\tau}C_j(i-1)\right)^{\theta_2(\tau)+1}\right)\right]\right\} \\
= \; & \sum_{j=1}^{J}\left\{\sum_{i=1}^{I^j}\left[-\theta_1+\theta_2\ln\left(a_{ij}+\theta_3 C_j(i)\right)\right]\right. \\
- \; & \left.\frac{\exp(-\theta_1)}{\theta_3(\theta_2+1)}\left[\sum_{i=1}^{I^j+1}\frac{1}{a_{ij}}\left(\left(a_{ij}+\theta_3C_j(i)\right)^{\theta_2+1}-\left(a_{ij}+\theta_3C_j(i-1)\right)^{\theta_2+1}\right)\right]\right\}
\end{aligned}
$$

with $\theta_1 := \theta_1(\tau)+\ln(\tau)$, $\theta_2 := \theta_2(\tau)$, and $\theta_3 := \frac{\theta_3(\tau)}{\tau}$. The last representation is again a version not depending on τ. Hence for different τ_0 and τ_* we get

$$
\begin{aligned}
&\theta_2(\tau_0) = \theta_2 = \theta_2(\tau_*), \\
&\frac{\theta_3(\tau_0)}{\tau_0} = \theta_3 = \frac{\theta_3(\tau_*)}{\tau_*} \Leftrightarrow \theta_3(\tau_0) = \theta_3(\tau_*)\frac{\tau_0}{\tau_*}, \\
&\theta_1(\tau_0)+\ln(\tau_0) = \theta_1 = \theta_1(\tau_*)+\ln(\tau_*) \Leftrightarrow \theta_1(\tau_0) = \theta_1(\tau_*)+\ln(\tau_*)-\ln(\tau_0).
\end{aligned}
$$

7 Additional details of the proofs

Additional details of the proof of Theorem II.1. The detailed derivation of $\int_0^{\tau_j} \lambda_j^A(t)dt$ for the model with additive damage accumulation follows by

$$
\begin{aligned}
\int_0^{\tau_j} \lambda_j^A(t)dt &= \int_0^{\tau_j} \frac{1}{\tau}\exp(-\theta_1)\left(a_j(t)+\theta_3\frac{1}{\tau}A_j(t)\right)^{\theta_2} dt \\
&= \sum_{i=1}^{I^j}\int_{t_{i-1,j}}^{t_{i,j}} \frac{\exp(-\theta_1)}{\tau}\left(a_{ij}+\theta_3\frac{1}{\tau}A_j(t)\right)^{\theta_2} dt \\
&\quad + \int_{t_{I^j,j}}^{\tau_j} \frac{\exp(-\theta_1)}{\tau}\left(a_{(I^j+1)j}+\theta_3\frac{1}{\tau}A_j(t)\right)^{\theta_2} dt \\
&= \frac{\exp(-\theta_1)}{\tau}\left[\sum_{i=1}^{I^j}\int_{t_{i-1,j}}^{t_{i,j}}\left(a_{ij}+\theta_3\frac{1}{\tau}\left[a_{ij}\left(t-\sum_{k=1}^{i-1}W_{kj}\right)+\sum_{k=1}^{i-1}a_{kj}W_{kj}\right]\right)^{\theta_2} dt\right. \\
&\quad \left.+ \int_{t_{I^j,j}}^{\tau_j}\left(a_{(I^j+1)j}+\theta_3\frac{1}{\tau}\left[a_{(I^j+1)j}\left(t-\sum_{k=1}^{I^j}W_{kj}\right)+\sum_{k=1}^{I^j}a_{kj}W_{kj}\right]\right)^{\theta_2} dt\right] \\
&= \frac{\exp(-\theta_1)\,\tau}{\tau\,\theta_3(\theta_2+1)}\left[\sum_{i=1}^{I^j}\frac{1}{a_{ij}}\left(a_{ij}+\theta_3\frac{1}{\tau}\left[a_{ij}\left(t-\sum_{k=1}^{i-1}W_{kj}\right)+\sum_{k=1}^{i-1}a_{kj}W_{kj}\right]\right)^{\theta_2+1}\Bigg|_{t_{i-1,j}}^{t_{i,j}}\right. \\
&\quad \left.+ \frac{1}{a_{(I^j+1)j}}\left(a_{(I^j+1)j}+\theta_3\frac{1}{\tau}\left[a_{(I^j+1)j}\left(t-\sum_{k=1}^{I^j}W_{kj}\right)+\sum_{k=1}^{I^j}a_{kj}W_{kj}\right]\right)^{\theta_2+1}\Bigg|_{t_{I^j,j}}^{\tau_j}\right] \\
&= \frac{\exp(-\theta_1)}{\theta_3(\theta_2+1)}\left[\sum_{i=1}^{I^j+1}\frac{1}{a_{ij}}\left(\left(a_{ij}+\theta_3\frac{1}{\tau}C_j(i)\right)^{\theta_2+1}-\left(a_{ij}+\theta_3\frac{1}{\tau}C_j(i-1)\right)^{\theta_2+1}\right)\right]
\end{aligned}
$$

with $W_{(I^j+1)j} := \tau_j - t_{I^j,j}$ and $C_j(i) = \sum_{k=1}^{i} a_{kj}W_{kj}$ for $i = 1,\dots,I^j+1$. □

Additional details of the proof of Corollary II.2. The intensity function λ_j^W of a load sharing model without damage accumulation satisfies

$$
\begin{aligned}
\int_0^{\tau_j} \lambda_j^W(t)dt &= \int_0^{\tau_j} \frac{1}{\tau}\exp(-\theta_1)a_j(t)^{\theta_2}\, dt \\
&= \sum_{i=1}^{I^j}\int_{t_{i-1,j}}^{t_{i,j}} \frac{\exp(-\theta_1)}{\tau}a_{ij}^{\theta_2}\, dt + \int_{t_{I^j,j}}^{\tau_j}\frac{\exp(-\theta_1)}{\tau}a_{(I^j+1)j}^{\theta_2}\, dt \\
&= \frac{\exp(-\theta_1)}{\tau}\left[\sum_{i=1}^{I^j}a_{ij}^{\theta_2}\,W_{ij}+a_{(I^j+1)j}^{\theta_2}(\tau_j-t_{I^j,j})\right] = \frac{\exp(-\theta_1)}{\tau}\left[\sum_{i=1}^{I^j+1}a_{ij}^{\theta_2}\,W_{ij}\right],
\end{aligned}
$$

so that, with $\lambda_j^W(t_{i,j}) = \frac{1}{\tau}\exp(-\theta_1)a_{ij}^{\theta_2}$, the form of the likelihood function L_W follows from formula $L = \left[\prod_{i=1}^{N(\tau)} \lambda(t_i)\right] \exp\left(-\int_0^\tau \lambda(t)dt\right)$ for the likelihood function of a general point process which was used in the proof of Theorem II.1.

To see also $\ln(L_W((\theta_1,\theta_2)^\top)) = \ln(L_M((\theta_1,\theta_2,0)^\top))$, note

$$C_j(i) - C_j(i-1) = \sum_{k=1}^{i} a_{kj}W_{kj} - \sum_{k=1}^{i-1} a_{kj}W_{kj} = a_{ij}W_{ij} \tag{3}$$

for $i = 1,\dots,I^j+1$, $j = 1,\dots,J$. Hence according to Theorem II.1, it holds

$$\begin{aligned}
&\ln(L_M((\theta_1,\theta_2,0)^\top)) \\
&= \sum_{j=1}^{J}\left\{\sum_{i=1}^{I^j}[-\theta_1+\theta_2\ln(a_{ij})-\ln(\tau)] - \frac{\exp(-\theta_1)}{\tau}\left[\sum_{i=1}^{I^j+1} a_{ij}^{\theta_2-1}\left(C_j(i)-C_j(i-1)\right)\right]\right\} \\
&= \sum_{j=1}^{J}\left\{\sum_{i=1}^{I^j}[-\theta_1+\theta_2\ln(a_{ij})-\ln(\tau)] - \frac{\exp(-\theta_1)}{\tau}\left[\sum_{i=1}^{I^j+1} a_{ij}^{\theta_2}\, W_{ij}\right]\right\} \\
&= \ln(L_W((\theta_1,\theta_2)^\top)).
\end{aligned}$$

To see $\ln(L_W((\theta_1,\theta_2)^\top)) = \lim_{\theta_3\to 0}\ln(L_A((\theta_1,\theta_2,\theta_3)^\top))$ note that L'Hospital's rule provides with (3)

$$\begin{aligned}
&\lim_{\theta_3\to 0}\frac{1}{\theta_3(\theta_2+1)}\frac{1}{a_{ij}}\left(\left(a_{ij}+\theta_3\frac{1}{\tau}C_j(i)\right)^{\theta_2+1} - \left(a_{ij}+\theta_3\frac{1}{\tau}C_j(i-1)\right)^{\theta_2+1}\right) \\
&= \lim_{\theta_3\to 0}\frac{1}{\theta_2+1}\frac{1}{a_{ij}}\left((\theta_2+1)\left(a_{ij}+\theta_3\frac{1}{\tau}C_j(i)\right)^{\theta_2}\frac{1}{\tau}C_j(i)\right. \\
&\qquad \left. -\ (\theta_2+1)\left(a_{ij}+\theta_3\frac{1}{\tau}C_j(i-1)\right)^{\theta_2}\frac{1}{\tau}C_j(i-1)\right) \\
&= \frac{1}{\tau}\frac{1}{a_{ij}}\left(a_{ij}^{\theta_2}C_j(i) - a_{ij}^{\theta_2}C_j(i-1)\right) = \frac{1}{\tau}\frac{1}{a_{ij}}a_{ij}^{\theta_2}a_{ij}W_{ij} = \frac{1}{\tau}a_{ij}^{\theta_2}W_{ij}
\end{aligned}$$

for $i = 1,\dots,I^j+1$. This implies $\ln(L_W((\theta_1,\theta_2)^\top)) = \lim_{\theta_3\to 0}\ln(L_A((\theta_1,\theta_2,\theta_3)^\top))$. $\square$

Proof of Lemma II.3. At first note

$$\begin{aligned}
&H_{ij}(t|t_{1,j},\dots,t_{i-1,j}) = \int_{t_{i-1,j}}^{t} -\frac{S'_{ij}(u|t_{1,j},\dots,t_{i-1,j})}{S_{ij}(u|t_{1,j},\dots,t_{i-1,j})}\,du \\
&= \int_{t_{i-1,j}}^{t} -\frac{\partial}{\partial u}\ln(S_{ij}(u|t_{1,j},\dots,t_{i-1,j}))\,du \\
&= -\ln(S_{ij}(t|t_{1,j},\dots,t_{i-1,j})) + \ln(S_{ij}(t_{i-1,j}|t_{1,j},\dots,t_{i-1,j})) \\
&= -\ln(S_{ij}(t|t_{1,j},\dots,t_{i-1,j})).
\end{aligned}$$

Additionally with $F_{ij}(t_{i-1,j}|t_{1,j},\ldots,t_{i-1,j}) := 1 - S_{ij}(t_{i-1,j}|t_{1,j},\ldots,t_{i-1,j})$, we get

$$\begin{aligned}
&P(F_{ij}(T_{i,j}|T_{1,j},\ldots,T_{i-1,j}) \leq t|T_{1,j}=t_{1,j},\ldots,T_{i-1,j}=t_{i-1,j}) \\
&\quad = P(F_{ij}(T_{i,j}|T_{1,j}=t_{1,j},\ldots,T_{i-1,j}=t_{i-1,j}) \leq t|T_{1,j}=t_{1,j},\ldots,T_{i-1,j}=t_{i-1,j}) \\
&\quad = P(T_{i,j} \leq F_{ij}^{-1}(t|T_{1,j}=t_{1,j},\ldots,T_{i-1,j}=t_{i-1,j})|T_{1,j}=t_{1,j},\ldots,T_{i-1,j}=t_{i-1,j}) \\
&\quad = F_{ij}(F_{ij}^{-1}(t|T_{1,j}=t_{1,j},\ldots,T_{i-1,j}=t_{i-1,j})|T_{1,j}=t_{1,j},\ldots,T_{i-1,j}=t_{i-1,j}) = t
\end{aligned}$$

so that the conditional distribution of $F_{ij}(T_{i,j}|T_{1,j},\ldots,T_{i-1,j})$ given $T_{1,j} = t_{1,j},\ldots,T_{i-1,j} = t_{i-1,j}$ is a uniform distribution on $[0,1]$. Hence the conditional distribution of $S_{ij}(T_{i,j}|T_{1,j},\ldots,T_{i-1,j})$ is also a uniform distribution on $[0,1]$. This implies

$$\begin{aligned}
&P(H_{ij}(T_{i,j}|T_{1,j},\ldots,T_{i-1,j}) \leq t|T_{1,j}=t_{1,j},\ldots,T_{i-1,j}=t_{i-1,j}) \\
&\quad = P(-\ln(S_{ij}(T_{i,j}|T_{1,j},\ldots,T_{i-1,j})) \leq t|T_{1,j}=t_{1,j},\ldots,T_{i-1,j}=t_{i-1,j}) \\
&\quad = P(S_{ij}(T_{i,j}|T_{1,j},\ldots,T_{i-1,j}) \leq \exp(-t)|T_{1,j}=t_{1,j},\ldots,T_{i-1,j}=t_{i-1,j}) \\
&\quad = \exp(-t)
\end{aligned}$$

which means that the conditional distribution of $H_{ij}(T_{i,j}|T_{1,j},\ldots,T_{i-1,j})$ given $T_{1,j} = t_{1,j},\ldots,T_{i-1,j} = t_{i-1,j}$ is an exponential distribution with parameter 1. □

Proof of Theorem II.4. Similarly as in the proof Theorem II.1, we get for the load sharing model with multiplicative damage accumulation

$$\begin{aligned}
\Lambda_{ij}^{M}(t) &= \int_{t_{i-1,j}}^{t} \lambda_j^M(u)du = \int_{t_{i-1,j}}^{t} \frac{1}{\tau}\exp(-\theta_1)a_j(u)^{\theta_2}A(u)^{\theta_3}\,du \\
&= \frac{\exp(-\theta_1)}{\tau}\frac{a_{ij}^{\theta_2}}{\tau^{\theta_3}}\int_{t_{i-1,j}}^{t}\left(a_{ij}\left(u-\sum_{k=1}^{i-1}W_{kj}\right)+\sum_{k=1}^{i-1}a_{kj}W_{kj}\right)^{\theta_3}du \\
&= \frac{\exp(-\theta_1)}{\tau}\frac{a_{ij}^{\theta_2}}{\tau^{\theta_3}\,a_{ij}(\theta_3+1)}\left(a_{ij}\left(u-t_{i-1,j}\right)+C_j(i-1)\right)^{\theta_3+1}\Big|_{t_{i-1,j}}^{t} \\
&= \frac{\exp(-\theta_1)\,a_{ij}^{\theta_2-1}}{\tau^{\theta_3+1}\,(\theta_3+1)}\left[\left(a_{ij}\left(t-t_{i-1,j}\right)+C_j(i-1)\right)^{\theta_3+1}-C_j(i-1)^{\theta_3+1}\right] \\
&= \frac{\exp(-\theta_1)\,a_{ij}^{\theta_2-1}}{\tau^{\theta_3+1}\,(\theta_3+1)}\left[\left(a_{ij}t-a_{ij}t_{i-1,j}+C_j(i-1)\right)^{\theta_3+1}-C_j(i-1)^{\theta_3+1}\right].
\end{aligned}$$

This is of the form

$$K(t) \;:=\; c\left[(at+b)^v-d\right] \tag{4}$$

which has the following inverse

$$K^{-t}(y) = \frac{1}{a}\left[\left(\frac{y}{c}+d\right)^{\frac{1}{v}}-b\right]. \tag{5}$$

This implies

$$(\Lambda_{ij}^{M})^{-1}(y)$$

$$= \frac{1}{a_{ij}} \left[\left(\frac{\tau^{\theta_3+1}(\theta_3+1)}{\exp(-\theta_1)\, a_{ij}^{\theta_2-1}} y + C_j(i-1)^{\theta_3+1} \right)^{\frac{1}{\theta_3+1}} + a_{ij} t_{i-1,j} - C_j(i-1) \right].$$

The load sharing model with additive damage accumulation satisfies

$$\begin{aligned}
\Lambda_{ij}^A(t) &= \int_{t_{i-1,j}}^t \lambda_j^A(u)du = \int_{t_{i-1,j}}^t \frac{1}{\tau} \exp(-\theta_1)(a_j(u) + \theta_3 A(u))^{\theta_2}\, du \\
&= \frac{\exp(-\theta_1)}{\tau} \int_{t_{i-1,j}}^t \left(a_{ij} + \theta_3 \frac{1}{\tau} \left[a_{ij} \left(u - \sum_{k=1}^{i-1} W_{kj} \right) + \sum_{k=1}^{i-1} a_{kj} W_{kj} \right] \right)^{\theta_2} du \\
&= \frac{\exp(-\theta_1)}{\theta_3(\theta_2+1)} \frac{1}{a_{ij}} \left(a_{ij} + \theta_3 \frac{1}{\tau} \left[a_{ij}(u - t_{i-1,j}) + C_j(i-1) \right] \right)^{\theta_2+1} \Bigg|_{t_{i-1,j}}^t \\
&= \frac{\exp(-\theta_1)}{\theta_3(\theta_2+1) a_{ij}} \left[\left(a_{ij} + \theta_3 \frac{1}{\tau} \left[a_{ij}(t - t_{i-1,j}) + C_j(i-1) \right] \right)^{\theta_2+1} \right. \\
&\quad - \left. \left(a_{ij} + \theta_3 \frac{1}{\tau} C_j(i-1) \right)^{\theta_2+1} \right] \\
&= \frac{\exp(-\theta_1)}{\theta_3(\theta_2+1) a_{ij}} \left[\left(\frac{\theta_3 a_{ij}}{\tau} t + a_{ij} - \frac{\theta_3}{\tau} \left[a_{ij} t_{i-1,j} - C_j(i-1) \right] \right)^{\theta_2+1} \right. \\
&\quad - \left. \left(a_{ij} + \theta_3 \frac{1}{\tau} C_j(i-1) \right)^{\theta_2+1} \right].
\end{aligned}$$

This has again the form (4) so that the inverse is given by (5) implying

$$\begin{aligned}
&(\Lambda_{ij}^A)^{-1}(y) \\
&\quad = \frac{\tau}{\theta_3 a_{ij}} \left[\left(\frac{\theta_3(\theta_2+1) a_{ij}}{\exp(-\theta_1)} y + \left(a_{ij} + \theta_3 \frac{1}{\tau} C_j(i-1) \right)^{\theta_2+1} \right)^{\frac{1}{\theta_2+1}} \right. \\
&\qquad - \left. a_{ij} + \frac{\theta_3}{\tau} \left[a_{ij} t_{i-1,j} - C_j(i-1) \right] \right]. \square
\end{aligned}$$

Proof of (11) and (12). The proofs of (11) and (12) are similar so that only the proof of (12) is given. Here, we get again with L'Hospital's rule

$$\begin{aligned}
&\lim_{\theta_3 \to 0} (\Lambda_{ij}^A)^{-1}(y) \\
&= \lim_{\theta_3 \to 0} \frac{\tau}{a_{ij}} \left[\frac{1}{\theta_2+1} \left(\frac{\theta_3(\theta_2+1) a_{ij}}{\exp(-\theta_1)} y + \left(a_{ij} + \theta_3 \frac{1}{\tau} C_j(i-1) \right)^{\theta_2+1} \right)^{\frac{1}{\theta_2+1}-1} \right. \\
&\qquad \cdot \left(\frac{(\theta_2+1) a_{ij}}{\exp(-\theta_1)} y + (\theta_2+1) \left(a_{ij} + \theta_3 \frac{1}{\tau} C_j(i-1) \right)^{\theta_2} \cdot \frac{1}{\tau} C_j(i-1) \right) \\
&\quad + \left. \frac{1}{\tau} \left[a_{ij} t_{i-1,j} - C_j(i-1) \right] \right]
\end{aligned}$$

$$
\begin{aligned}
&= \frac{\tau}{a_{ij}}\left[\frac{1}{\theta_2+1}\left((a_{ij})^{\theta_2+1}\right)^{\frac{-\theta_2}{\theta_2+1}}\cdot\left(\frac{(\theta_2+1)a_{ij}}{\exp(-\theta_1)}y+(\theta_2+1)\,(a_{ij})^{\theta_2}\cdot\frac{1}{\tau}\,C_j(i-1)\right)\right.\\
&\quad\left. +\ \frac{1}{\tau}\left[a_{ij}t_{i-1,j}-C_j(i-1)\right]\right]\\
&= \frac{\tau}{a_{ij}}\left[(a_{ij})^{-\theta_2}\cdot\left(\frac{a_{ij}}{\exp(-\theta_1)}y+(a_{ij})^{\theta_2}\cdot\frac{1}{\tau}\,C_j(i-1)\right)+\frac{1}{\tau}\left[a_{ij}t_{i-1,j}-C_j(i-1)\right]\right]\\
&= \frac{1}{a_{ij}}\left[\frac{\tau\ a_{ij}}{\exp(-\theta_1)a_{ij}^{\theta_2}}y+\ C_j(i-1)+a_{ij}t_{i-1,j}-C_j(i-1)\right]\\
&= \frac{\tau}{\exp(-\theta_1)\,a_{ij}^{\theta_2}}y+t_{i-1,j}.\square
\end{aligned}
$$

References

Leckey, K., Müller, C. H., Szugat, S., and Maurer, R. (2020). Prediction intervals for load sharing systems in accelerated life testing. *Quality and Reliability Engineering International*, 36(6):1895–1915.